


# A Floquet theory-based fast time-domain stability analysis for $N$ -parallel inverters system

Hong Li<sup>1</sup>  | Xiaoheng Jiang<sup>1</sup> | Chen Liu<sup>2</sup> | Zhong Li<sup>3,4</sup> | Leopoldo G. Franquelo<sup>5</sup> | Sergio Vazquez<sup>5</sup>

<sup>1</sup> School of Electrical Engineering, Beijing Jiaotong University, Beijing, China

<sup>2</sup> Langfang Power Supply Company, State Grid Jibei Electric Power Co. LTD, Beijing, China

<sup>3</sup> School of Mathematics and Statistics, Minnan Normal University, Zhangzhou, China

<sup>4</sup> Faculty of Mathematics and Computer Science, Fernuniversität in Hagen, Hagen, Germany

<sup>5</sup> Department of Electronic Engineering, University of Seville, Seville, Spain

## Correspondence

Hong Li, School of Electrical Engineering, Beijing Jiaotong University, Beijing, China.  
Email: hli@bjtu.edu.cn

## Funding information

National Natural Science Foundation of China, Grant/Award Number: U1866211; General Programs of the National Natural Science Foundation of China, Grant/Award Numbers: 51577010, 51777012; Fujian Provincial Natural Science Foundation, Grant/Award Number: 2020J01800; Excellent Youth Scholars of National Natural Science Foundation of China, Grant/Award Number: 51822701

## Abstract

Based on Floquet theory, a simple and fast time-domain stability analysis method for an  $N$ -parallel inverters system is proposed. Furthermore, a general time-domain model of the  $N$ -parallel inverters system in grid-connected mode and in island mode are derived, and the corresponding stability criteria are derived based on the Floquet theory. Subsequently, simulations and experiments of a two-parallel inverters system in island and grid-connected modes are conducted to verify the correctness and effectiveness of the proposed time-domain stability analysis method. To the end, the complexity comparison between the proposed time-domain method and the traditional frequency-domain method is presented to prove the advantages of the proposed method over the tedious manual derivation.

## 1 | INTRODUCTION

The voltage source inverter (VSI) enables the power transfer from a renewable energy sources (RES) to the grid [1], where the LCL filter single-phase inverters system is usually used in VSI to limit the switching current ripple [2, 3]. As the interface between renewable energy generators and an AC grid, inverters usually adopt parallel structure to inject energy into the grid [4–7]. However, due to the system bus, the dynamic interactions between complexly coupled inverters exists [8], which leads the system to have several resonance frequencies [9]. On the other hand, the required additional current-sharing control to the parallel inverters system may increase the coupling strength

among the inverter modules and in turn strengthen the interaction among them, which should also be considered in the system design. Once the main circuit or control parameters are set improperly, this interaction may cause the system to oscillate or even collapse, and with the rapid development of AC–DC hybrid micro grids, these oscillations or collapse phenomenon occur more and more frequently; therefore, the modelling and stability analysis of  $N$ -parallel inverters systems have become an urgent problem for theorists and engineers [10], and the prior stability analysis for  $N$ -parallel inverters system is of practical significance.

Up to now, the stability analysis methods used for parallel inverters system are mainly in frequency domain. For example,

This is an open access article under the terms of the [Creative Commons Attribution-NonCommercial-NoDerivs](https://creativecommons.org/licenses/by-nc-nd/4.0/) License, which permits use and distribution in any medium, provided the original work is properly cited, the use is non-commercial and no modifications or adaptations are made.

© 2021 The Authors. *IET Power Electronics* published by John Wiley & Sons Ltd on behalf of The Institution of Engineering and Technology

stability analysis methods based on impedance criterion have been widely applied for inverters systems [11–16]. However, in practical applications, as the number of inverters in the parallel system increases, or the circuit parameters of each inverter are variant, the derivation of the impedance criterion becomes quite complicated, leading to rare research on modelling and stability analysis of an  $N$ -parallel inverters system (especially for  $N \geq 3$ ), to our best knowledge. In [17], it has been proved that the complexity of modelling the multi-stage DC–DC converters system in the frequency-domain will increase exponentially versus the number of the DC–DC converters according to the manual derivation process. Hence, the impedance modelling and prediction methods based on the black-box modelling was proposed in [18]; however, since it only uses terminal characteristics and does not pay attention to the inner parameters of the inverters, once deviations occur, it is difficult to correct it, so that the accuracy and the correctness of these methods are difficult to be ensured in practice. On the other hand, the impedance criterion only provides the sufficient condition for the stability of the parallel inverters system, which is usually very conservative for real applications [19, 20].

To avoid the conservation and complexity of impedance criterion method, the Routh criterion is also widely used for judging the stability of inverters as sufficient and necessary condition [21, 22]. To use Routh criterion, the closed-loop transfer function of the inverter system should be first derived and then it need be further simplified to obtain the closed loop characteristic equation and the effective stability criterion. However, for an  $N$ -parallel inverters system ( $N > 2$ ), its closed-loop transfer function is a complex high-order polynomial, and the expression of the high-order polynomial will become much more complicated with the increase of the number of paralleled inverters. Therefore, the simplified closed loop characteristic equation for  $N$ -parallel inverters system ( $N > 2$ ) is difficult to obtain; even if obtained, its accuracy can hardly satisfy the requirement in real applications.

Besides, the state-space-based analysis method is also a tool to analyse harmonic stability for inverters, which can explain the resonance phenomenon in inverters [23–25]. However, unlike three-phase inverters, the steady-state AC variables of a single-phase inverter cannot be expressed into a DC form by the coordinate transformation [26], which leads the state-space-based analysis method not be able to be used into single-phase inverters directly.

In recent years, a time-domain stability analysis method based on Floquet theory has been proposed and successfully employed into DC–DC converters system and single-phase inverter with proportional integral (PI) control and proportional resonance (PR) control [22, 27–30]. Compared with frequency-domain stability analysis method, the time-domain stability analysis method based on Floquet theory can avoid the complicated derivation of the required transfer functions in Routh criterion or the impedances expression in impedance criterion, only a state transition matrix is required, which can be obtained by the time-domain state equations for power converters system. Further, the stability analysis can be analysed by computer-aided

way, which provides a possible method for the stability analysis for an  $N$ -parallel inverters system.

Although Floquet theory has been employed into the stability analysis for single inverter with only PI or PR control, it cannot be directly applied into the  $N$ -parallel inverters system, since there is the interaction among the inverter modules and the double closed-loop control is used in the  $N$ -parallel inverters system due to the necessary current-sharing outer control. Furthermore, it is a challenging problem on how to bring the additional current-sharing control to the time-domain stability analysis method, as it is associated with system bus and does not appear in state variable of each inverter module.

Therefore, this paper proposed a new time-domain stability analysis method for  $N$ -parallel inverters system based on Floquet theory, which can be used to reduce complex manual derivation and the high time cost in frequency-domain stability analysis methods. The rest of this paper is organised as follows: in Section 2, the general time-domain model of the  $N$ -parallel inverters system is established based on Floquet theory, both for grid-connected mode and for island mode. And the corresponding stability criterion of the  $N$ -parallel inverters system is derived. In Section 3, a two-parallel inverters system is taken as an example, its stability has been analysed, both in grid-connected mode and in island mode. In Section 4, the correctness of the stability analysis results in Section 3 are verified by simulation and experiment results. In Section 5, the complexity of the frequency-domain and the proposed time-domain stability analysis methods are compared. Finally, the conclusion is drawn.

## 2 | THE TIME-DOMAIN MODEL OF $N$ -PARALLEL INVERTERS SYSTEM BASED ON FLOQUET THEORY

### 2.1 | Floquet theory

Floquet theory is used to judge the stability of periodic systems [27]. According to the zero-solution condition of the perturbation equation, the stable of system can be uniquely determined.

Assume a periodic system (1), and its steady-state periodic solution is noted as  $X$ ; thus  $X(t) = X(t+T)$ , where,  $T$  is the period of the steady-state periodic solution.

$$\dot{x} = G(t, x). \quad (1)$$

When the system suffers a small perturbation  $\delta(t)$  at the steady-state periodic solution  $X$ , the state variables at the steady-state periodic solution can be expressed as

$$x(t) = X + \delta(t). \quad (2)$$

Substituting (2) into (1), and linearising by the Taylor series expansion, the perturbation equation can be obtained, as shown

in (3), where  $E(t)$  is the Jacobi matrix of the system.

$$\frac{d\delta(t)}{dt} \approx G'(t, X) \delta(t) = E(t) \delta(t) = J(t, X) \delta(t). \quad (3)$$

According to the Floquet theory, there is  $E(t) = E(t+T)$ , since the system is a periodic system. Then, assuming that  $V(t)$  is a basic solution matrix of the system (3), there must be a non-singular matrix  $\Phi(t) = \Phi(t+T)$  and a constant matrix  $D$ , so that  $V(t)$  can be expressed as  $V(t) = \Phi(t)e^{tD}$ . Further, (4) can be deduced.

$$V'(t+T) = E(t+T)V(t+T) = E(t)V(t+T). \quad (4)$$

Therefore,  $V(t+T)$  is also the basic solution matrix of the system (3). According to the uniqueness of the basic solution matrix, there is  $V(t+T) = CV(t)$ . It should be noticed that the matrices  $V(t)$  and  $V(t+T)$  have the following relationship:

$$V(t+T) = \Phi(t+T)e^{(t+T)D} = \Phi(t)e^{tD}e^{TD} = V(t)e^{TD}. \quad (5)$$

Thus,  $C$  can be got as (6), where  $C$  is a reversible matrix. Specially, if  $E(t)$  is a constant matrix, it can be chosen as the matrix  $D$ .

$$C = e^{TD}. \quad (6)$$

On the other hand, assume  $\varepsilon_i$  to be the disturbance factor and there is a small perturbation at  $t_0$  moment, then combining the disturbance component of the system  $v(t_0) = V(t_0)\varepsilon_i$ , with (5) and (6) results in

$$\begin{aligned} S &= \frac{\|v(t_0 + nT)\|}{\|v(t_0)\|} = \frac{\|V(t_0)C^n \varepsilon_i\|}{\|V(t_0)\varepsilon_i\|} \\ &\leq \frac{\|V(t_0)\varepsilon_i\| \|C^n\|}{\|V(t_0)\varepsilon_i\|} = \|C^n\|, \end{aligned} \quad (7)$$

where  $S$  stands for the perturbation transfer function and the necessary and sufficient conditions for the stability of the system depend on

$$\lim_{n \rightarrow \infty} \|C^n\| = 0. \quad (8)$$

According to the norm theorem, there is

$$\lim_{n \rightarrow \infty} \|C^n\| = 0 \Leftrightarrow |\lambda_{\max}| < 1, \quad (9)$$

where  $|\lambda_{\max}| = \max\{|\lambda_i|, i = 1, 2, 3, \dots\}$ ,  $\lambda_{\max}$  is called the spectral radius of matrix  $C$  and  $\lambda_i, i = 1, 2, 3, \dots$  are the eigenvalues of matrix  $C$ .

In summary, according to the Floquet theory, the stability of the system can be described in details:

- If  $|\lambda_{\max}| < 1$ , the system is stable;
- Otherwise, the system is unstable.

Due to the  $N$ -parallel inverters with PR control is a periodic system, its stability can be judged by the stability criterion based on Floquet theory in time domain.

## 2.2 | The general time-domain model of $N$ -parallel inverters system

PR control was firstly proposed by Marco Liserre in 2006 to provide an optimal ac current control for inverters [30], which can offer infinite gain at a certain frequency by using generalised integrators and obtain zero steady-state error at the fundamental frequency. Therefore, the PR control is adopted to achieve current control in this paper.

It should also be noticed that the required current-sharing control in the parallel inverters system might reduce the system's stability [31], so that the additional current-sharing control also needs to be considered in modelling. Although the droop control method is usually used to achieve current and power balance among the inverter modules [18,32,33], its dynamic performance is poor because of the quite low bandwidth of droop control [18]. The average current control method is commonly used as an alternative method when inverters operate in parallel, and it can better achieve power balance and ensure the quality of the voltage or current and is useful in high-performance applications in AC distributed systems [34]. Hence, the average current control is adopted to achieve current-sharing and the corresponding time-domain model is established in this paper.

Although the grid-connected inverter with reactive power capability are done some research [35–37], the grid-connected inverters with unity power factor are more common in real applications, therefore, the grid-connected inverters system with unit power factor is taken as the example in this paper.

According to the above mentioned, the circuit model of the  $N$ -parallel single-phase inverters system in grid-connected mode is firstly established, as shown in Figure 1. The current sharing link adopts instantaneous current average control and the current loops of each inverter adopt PR control and use the same current reference signal. In addition,  $N$  is the number of inverters in the system and the meanings of the other symbols are shown in Table 1.

Subsequently, for the  $j$ th inverter ( $j = 1, 2, \dots, N$ ) in Figure 1, the state Equation (10) of the main circuit can be obtained according to Kirchhoff current laws (KCL) and Kirchhoff voltage laws (KVL).

$$\begin{cases} \frac{du_{Cj}}{dt} = \frac{1}{C_j} i_{1-j} - \frac{1}{C_j} i_{2-j} \\ \frac{di_{1-j}}{dt} = \frac{U_{dj}}{L_{1-j}} i_{mj} - \frac{R_{1-j} + R_{dj}}{L_{1-j}} i_{1-j} + \frac{R_{dj}}{L_{1-j}} i_{2-j} - \frac{u_{Cj}}{L_{1-j}} \\ \frac{di_{2-j}}{dt} = \frac{1}{L_{2-j}} u_{Cj} + \frac{R_{dj}}{L_{2-j}} i_{1-j} - \frac{R_{2-j} + R_{dj}}{L_{2-j}} i_{2-j} - \frac{u_s}{L_{2-j}}, \\ i_s = \sum_{j=1}^N (i_{2-j}) \end{cases}, \quad (10)$$

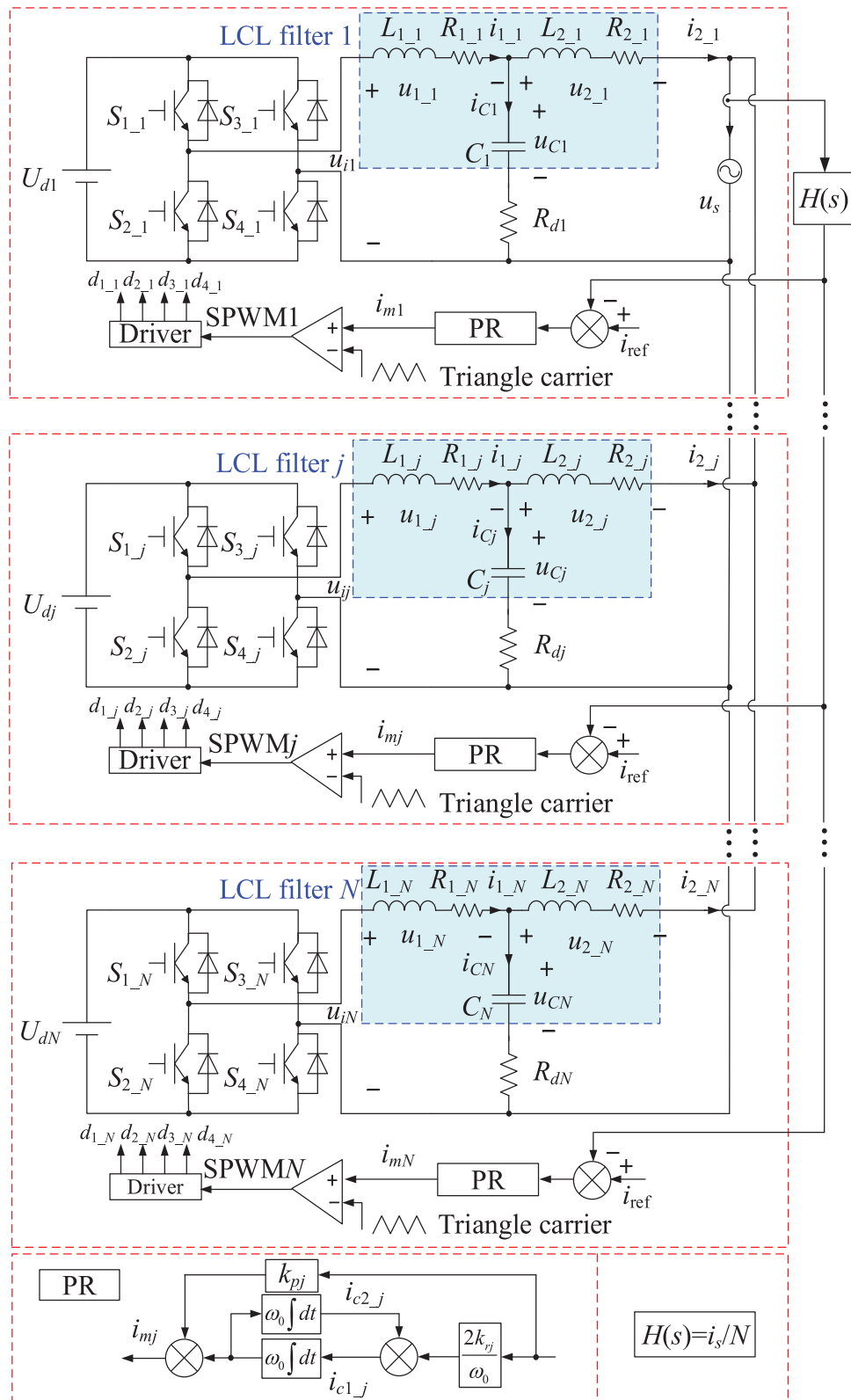


FIGURE 1 The circuit model of the  $N$ -parallel inverters system in grid-connected mode

**TABLE 1** Index of symbols in Figure 1

Symbol	Index
$U_{dj}$	DC voltage source of the $j$ th inverter
$u_{ij}$	output voltage of H-bridge of the $j$ th inverter
$L_{1-j}$	inverter-side inductance of the $j$ th inverter
$R_{1-j}$	parasitic resistance of $L_{1-j}$
$L_{2-j}$	grid-side inductance of the $j$ th inverter
$R_{2-j}$	parasitic resistance of $L_{2-j}$
$i_{1-j}$	inverter-side inductor current of the $j$ th inverter
$i_{2-j}$	grid-side inductor current of the $j$ th inverter
$u_{1-j}$	voltage of $L_{1-j}$ and $R_{1-j}$ of the $j$ th inverter
$u_{2-j}$	voltage of $L_{2-j}$ and $R_{2-j}$ of the $j$ th inverter
$C_j$	filter capacitor of the $j$ th inverter
$R_{dj}$	the additional damping resistor
$u_{Cj}$	voltage of capacitor of the $j$ th inverter
$u_s$	grid voltage
$i_s$	grid current
$i_{\text{ref}}$	the closed-loop reference current
$e_j$	the difference between the output current of the $j$ th inverter and the closed-loop reference current
$i_{mj}$	the output signal of the PR controller
$d_{1-j}-d_{4-j}$	duty signals of the four switches of the $j$ th inverter

In the control circuit, since the PR controller is a second-order system, in addition to selecting  $i_{mj}$  as the state variable for the  $j$ th inverter, one more state variable should be selected. The state variable can be arbitrarily selected in the PR control block diagram.

For convenience of calculation,  $i_{c1-j}$  is selected as the system state variable. Also, the average current control that strengthens the coupling interaction with other modules is considered, as this current loop collects the output current of all inverters and feeds the sum of current back to each module.

According to Figure 1, the expression of the state variable in the control circuit of the  $j$ th inverter can be obtained as (11).

$$\begin{cases} i_{mj} = \omega_0 \int (i_{c1-j}) dt + k_{pj} \left( i_{\text{ref}} - \frac{i_s}{N} \right) \\ i_{c1-j} = \frac{2k_{rj}}{\omega_0} \left( i_{\text{ref}} - \frac{i_s}{N} \right) - \omega_0 \int \left[ i_{mj} - k_{pj} \left( i_{\text{ref}} - \frac{i_s}{N} \right) \right] dt \end{cases} \quad (11)$$

Therefore, one has

$$\begin{cases} \frac{di_{mj}}{dt} = \omega_0 \cdot i_{c1-j} + k_{pj} \cdot \frac{di_{\text{ref}}}{dt} - \frac{k_{pj}}{N} \cdot \frac{di_s}{dt} \\ \frac{di_{c1-j}}{dt} = \frac{2k_{rj}}{\omega_0} \cdot \frac{di_{\text{ref}}}{dt} - \frac{2k_{rj}}{\omega_0 N} \cdot \frac{di_s}{dt} \\ - \omega_0 \left[ i_{mj} - k_{pj} \left( i_{\text{ref}} - \frac{i_s}{N} \right) \right] \end{cases}, \quad (12)$$

Substituting (10) into (12) and using state variables  $i_{2-1}, \dots, i_{2-j}, \dots, i_{2-N}$  to decouple the sum of current  $i_s$ , result in (13).

$$\begin{cases} \frac{di_{mj}}{dt} = -\frac{k_{pj}}{N} \sum_{k=1}^N \left( \frac{1}{L_{2-k}} u_{Ck} + \frac{R_{dk}}{L_{2-k}} i_{1-k} \right) + \omega_0 \cdot i_{c1-k} \\ + k_{pj} \cdot \frac{di_{\text{ref}}}{dt} \\ \frac{di_{c1-j}}{dt} = -\frac{2k_{rj}}{\omega_0 N} \sum_{k=1}^N \left( \frac{1}{L_{2-k}} u_{Ck} + \frac{R_{dk}}{L_{2-k}} i_{1-k} \right) - \omega_0 i_{mj} \\ + \frac{\omega_0 k_{pj}}{N} \sum_{k=1}^N (i_{2-k}) + \omega_0 k_{pj} i_{\text{ref}} + \frac{2k_{rj}}{\omega_0} \cdot \frac{di_{\text{ref}}}{dt} \end{cases}, \quad (13)$$

According to (10) and (13), selecting  $u_{C1}, i_{1-1}, i_{2-1}, i_{m1}, i_{c1-1}, \dots, u_{Cj}, i_{1-j}, i_{2-j}, i_{mj}, i_{c1-j}, \dots, u_{CN}, i_{1-N}, i_{2-N}, i_{mN}$  and  $i_{c1-N}, j = 1, 2, \dots, N$ , as the state variables of the system, the state expression of the  $N$ -parallel inverters system in grid-connected mode can be obtained. Furthermore, the Jacobi matrix  $E_{sN}(t)$  of the inverters system can be written as

$$E_{sN}(t) = \begin{bmatrix} B_{11} & B_{12} & B_{13} & \cdots & B_{1N} \\ B_{21} & B_{22} & B_{23} & \cdots & B_{2N} \\ B_{31} & B_{32} & B_{33} & \cdots & B_{3N} \\ \vdots & \vdots & \vdots & \ddots & \vdots \\ B_{N1} & B_{N2} & B_{N3} & \cdots & B_{NN} \end{bmatrix}, \quad (14)$$

$E_{sN}(t)$  is a  $5N$ th order matrix and consists of sub-matrices  $B_{kj}(k, j = 1, 2, \dots, N)$ . In (14),  $B_{jj}$  represents the self-action matrix of each inverter, as shown in (15), which is caused by the main circuit of each module;  $B_{kj}(k, j = 1, 2, \dots, N; k \neq j)$  represents the interaction matrix between each module, as shown in (16), which is caused by the interaction among modules and the current-sharing control strategy.

Since the obtained Jacobi matrix  $E_{sN}(t)$  does not contain time variables, based on Floquet theory, there is  $D_{sN} = E_{sN}(t)$ . Then, the state transition matrix of the  $N$ -parallel inverters system in the grid-connect mode can be expressed as  $C_{sN} = e^{TD_{sN}}$ , where the time constant  $T$  is set as  $T = 1/50$ s as same as the period of inverter system. According to Floquet theory, the stability of the system is analyzed by calculating the modulus of the maximum eigenvalue of  $C_{sN} = e^{TD_{sN}}$ , namely,  $|\lambda_{\max}|$ :

- If  $|\lambda_{\max}| < 1$ , the system is stable;
- Otherwise, the system is unstable.

Furthermore, the imaginary part of the eigenvalue can represent the oscillation frequency.

$$B_{jj} (j = 1, 2, \dots, N) =$$

$$\begin{bmatrix} 0 & \frac{1}{C_j} & -\frac{1}{C_j} & 0 & 0 \\ \frac{1}{L_{1-j}} & -\frac{R_{1-j} + R_{dj}}{L_{1-j}} & \frac{R_{dj}}{L_{1-j}} & \frac{U_{dj}}{L_{1-j}} & 0 \\ \frac{1}{L_{2-j}} & \frac{R_{dj}}{L_{2-j}} & -\frac{R_{2-j} + R_{dj}}{L_{2-j}} & 0 & 0 \\ \frac{k_{pj}}{NL_{2-j}} & \frac{k_{pj}R_{dj}}{NL_{2-j}} & \frac{k_{pj}(R_{2-j} + R_{dj})}{NL_{2-j}} & 0 & \omega_0 \\ \frac{2k_{rj}}{\omega_0 NL_{2-j}} & \frac{2k_{rj}R_{dj}}{\omega_0 NL_{2-j}} & \frac{2k_{rj}(R_{2-j} + R_{dj})}{\omega_0 NL_{2-j}} & -\omega_0 & 0 \\ & & -\frac{\omega_0 k_{pj}}{N} & & \end{bmatrix}, \quad (15)$$

$$B_{kj} (k \neq j; k, j = 1, 2, \dots, N) =$$

$$\begin{bmatrix} 0 & 0 & 0 & 0 & 0 \\ 0 & 0 & 0 & 0 & 0 \\ 0 & 0 & 0 & 0 & 0 \\ \frac{k_{pk}}{NL_{2-j}} & \frac{k_{pk}R_{dj}}{NL_{2-j}} & \frac{k_{pk}(R_{2-j} + R_{dj})}{NL_{2-j}} & 0 & 0 \\ \frac{2k_{rk}}{\omega_0 NL_{2-j}} & \frac{2k_{rk}R_{dj}}{\omega_0 NL_{2-j}} & \frac{2k_{rk}(R_{2-j} + R_{dj})}{\omega_0 NL_{2-j}} & 0 & 0 \\ & & -\frac{\omega_0 k_{pk}}{N} & & \end{bmatrix}. \quad (16)$$

Similarly, this proposed method can be deduced and applied to an inverters system with similar structures, not only for the  $N$ -parallel inverters system in island mode, but also for the variation parameters PWM filters. Further, the proposed method can easy extend to  $N \geq 3$  paralleled inverters through (14).

And the theoretical stability analysis results, simulation and experimental results both in grid-connected mode and in island mode are given in Section 3.

**TABLE 2** The parameters in simulation and experiment of two parallel inverters system in grid-connected mode

Main circuit parameters	CONTROL PARAMETERS
$U_{d1} = 350 \text{ V}; L_{1-1} = 5.8 \text{ mH};$ $L_{2-1} = 1 \text{ mH}; C_1 = 1.5 \mu\text{F};$ $R_{1-1} = 0.01 \Omega; R_{2-1} = 0.01 \Omega;$ $R_{d1} = 4.5 \Omega;$	<b>Case I:</b> $k_{p1} = k_{p2} = 0.08\text{--}0.12;$ $k_{r1} = k_{r2} = 500;$
$U_{d2} = 350 \text{ V}; L_{1-2} = 5.8 \text{ mH};$ $L_{2-2} = 1 \text{ mH}; C_2 = 1.5 \mu\text{F};$ $R_{1-2} = 0.01 \Omega; R_{2-2} = 0.01 \Omega;$ $R_{d2} = 4.5 \Omega;$	<b>Case II:</b> $k_{p1} = k_{p2} = 0.09;$ $k_{r1} = k_{r2} = 500\text{--}600.$
$u_s = 220 \text{ V}$	

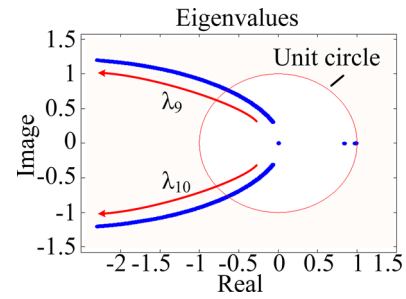


**FIGURE 2** Eigenvalues trend of  $C_{s2}$  when increasing  $k_{pj}$  and fixed  $k_{rj} = 500$

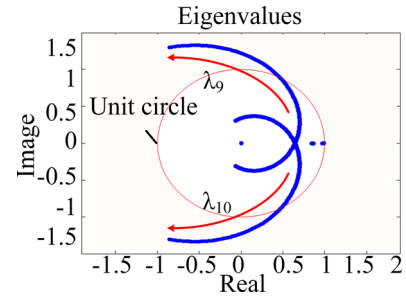


**FIGURE 3** Eigenvalues trend of  $C_{s2}$  when increasing  $k_{rj}$  and fixed  $k_{pj} = 0.09$

### 3 | STABILITY ANALYSIS BASED ON THE FLOQUET THEORY

#### 3.1 | The two-parallel inverters system in grid-connected mode

Here, a two-parallel inverters system in grid-connected mode is taken as an example. According to Section 2, when  $N = 2$ , we can be obtained the system state transition matrix  $C_{s2} = e^{TDs2}$ .

The parameters of the parallel inverters system in grid-connected mode is given in Table 2. The time-domain stability analysis results are presented with the change of the control parameters  $k_{pj}$  and  $k_{rj}$ . Figures 2 and 3 show the trend of eigenvalue changes with increasing the  $k_{pj}$  and  $k_{rj}$  parameters,

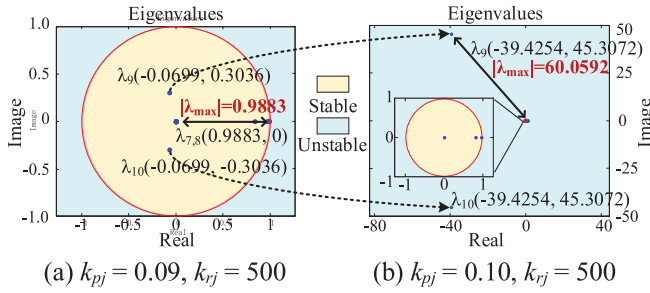


**FIGURE 4** Case I: Eigenvalue distribution of  $C_{s2}$  when  $k_{pj}$  changing. (a)  $k_{pj} = 0.09$ ,  $k_{rj} = 500$ . (b)  $k_{pj} = 0.10$ ,  $k_{rj} = 500$

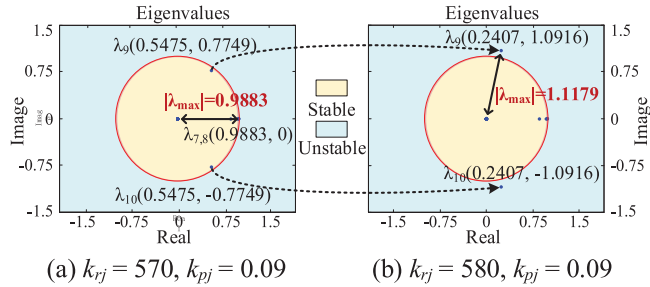


**FIGURE 5** Case II: Eigenvalue distribution of  $C_{s2}$  when  $k_{rj}$  changing. (a)  $k_{rj} = 570$ ,  $k_{pj} = 0.09$ . (b)  $k_{rj} = 580$ ,  $k_{pj} = 0.09$

respectively. It can be seen from Figures 2 and 3 that as the control parameters increase, the eigenvalues of the state transition matrix gradually pass out of the unit circle in the form of conjugates.

**Case I:** Stepwise increase  $k_{pj}(j = 1, 2)$ , when  $k_{pj}(j = 1, 2) = 0.09$ , as shown in Figure 4(a), the modulus of the maximum eigenvalue of the system state transition matrix  $C_{s2}$  is  $0.9883 < 1$ , which is within the unit circle. According to Floquet theory, system is stable.

When  $k_{pj}(j = 1, 2) = 0.10$ , as shown in Figure 4(b), the eigenvalue of the system state transition matrix  $C_{s2}$  partially exceeds the unit circle, and the modulus of the maximum eigenvalue is  $60.0592 > 1$ . According to Floquet theory, system is unstable.

**Case II:** Stepwise increase  $k_{rj}(j = 1, 2)$ , when  $k_{rj}(j = 1, 2) = 570$  as shown in Figure 5(a), the modulus of the maximum eigenvalue of the system state transition matrix  $C_{s2}$  is  $0.9883 < 1$ , which is within the unit circle. According to Floquet theory, system is stable.

When  $k_{rj}(j = 1, 2) = 580$ , as shown in Figure 5(b), the eigenvalue of the system state transition matrix  $C_{s2}$  partially exceeds the unit circle, and the modulus of the maximum eigenvalue is  $1.1179 > 1$ . According to Floquet theory, system is unstable.

### 3.2 | A two-parallel inverters system in island mode

Similarly, a two-parallel inverters system in island mode is taken as an example in Figure 6, to prove this stability analysis method is also suitable for system in island mode.

**TABLE 3** The parameters in simulation and experiment of two parallel inverters system in island mode

Main circuit parameters	CONTROL PARAMETERS
$U_{d1} = 350$ V; $L_{1,1} = 5.8$ mH;	$k_{p1} = k_{p2} = 0.08$ ;
$L_{2,1} = 1$ mH; $C_1 = 1.5$ $\mu$ F;	$k_{r1} = k_{r2} = 500$ ;
$R_{1,1} = 0.01$ $\Omega$ ; $R_{2,1} = 0.01$ $\Omega$ ;	<b>Case I:</b>
$R_{d1} = 4.3$ $\Omega$ ;	$k_{cp} = 0.010$ – $0.015$ ;
$U_{d2} = 350$ V; $L_{1,2} = 5.8$ mH;	$k_{ci} = 10$ ;
$L_{2,2} = 1$ mH; $C_2 = 1.5$ $\mu$ F;	<b>Case II:</b>
$R_{1,2} = 0.01$ $\Omega$ ; $R_{2,2} = 0.01$ $\Omega$ ;	$k_{cp} = 0.010$ ;
$R_{d2} = 4.3$ $\Omega$ ;	$k_{ci} = 15$ – $25$ .
$R_o = 100$ $\Omega$ , $u_o = 220$ V	

The controls of system adopt the voltage and current double-loop control strategy, the outer voltage loop uses PI control, the inner current loop applies PR control, and each inverter takes the same current reference signal.  $R_o$  is the load resistance,  $u_o$  is the output voltage,  $u_{ref}$  is the closed-loop reference voltage and  $i_{ref}$  is the closed-loop reference current of PI controller output, the rest of the symbols are the same as Table 1.

According to Section 2, when  $N = 2$ , the system state transition matrix can be obtained as  $C_2 = e^{TD_2}$ . The time-domain stability analysis results are presented with the change of the control parameters  $k_{cp}$  and  $k_{ci}$ . Figures 7 and 8 show the trend of eigenvalue changes with increasing the  $k_{cp}$  and  $k_{ci}$  parameters, respectively. The parameters of the parallel inverters system in island mode are given in Table 3.

**Case I:** Stepwise increase  $k_{cp}$ , as can be obtained from Figure 9(a), when  $k_{cp} = 0.011$ , the modulus of the maximum eigenvalue of the system state transition matrix  $C_2$  is  $0.8576 < 1$ , which is located in the unit circle. According to Floquet theory, the system is stable.

As shown in Figure 9(b), when  $k_{cp}$  increases to  $0.012$ , the eigenvalue of the 1qstate transition matrix  $C_2$  partially exceeds the unit circle, and the modulus of the maximum eigenvalue is  $3.1282 > 1$ . According to Floquet theory, system is unstable.

**Case II:** Stepwise increase  $k_{ci}$ , as can be obtained from Figure 10(a), when  $k_{ci} = 17$ , the modulus of the maximum eigenvalue of the system state transition matrix  $C_2$  is  $0.9867 < 1$ , which is located in the unit circle. According to Floquet theory, the system is stable.

As shown in Figure 10(b), when  $k_{ci}$  increases to  $18$ , the eigenvalue of the system state transition matrix  $C_2$  partially exceeds the unit circle, and the modulus of the maximum eigenvalue is  $1.2680 > 1$ . According to Floquet theory, system is unstable.

## 4 | SIMULATION AND EXPERIMENT

### 4.1 | Simulation results

#### 4.1.1 | The two-parallel inverters system in grid-connected mode

**Case I:** As shown in Figure 11, when  $k_{pj}(j = 1, 2) = 0.09$ , the grid-connected current of the two inverters tends to be

**FIGURE 6** The circuit model of the  $N$ -parallel inverters system in island mode

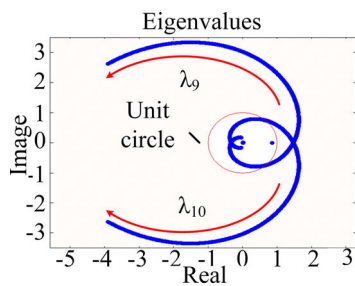
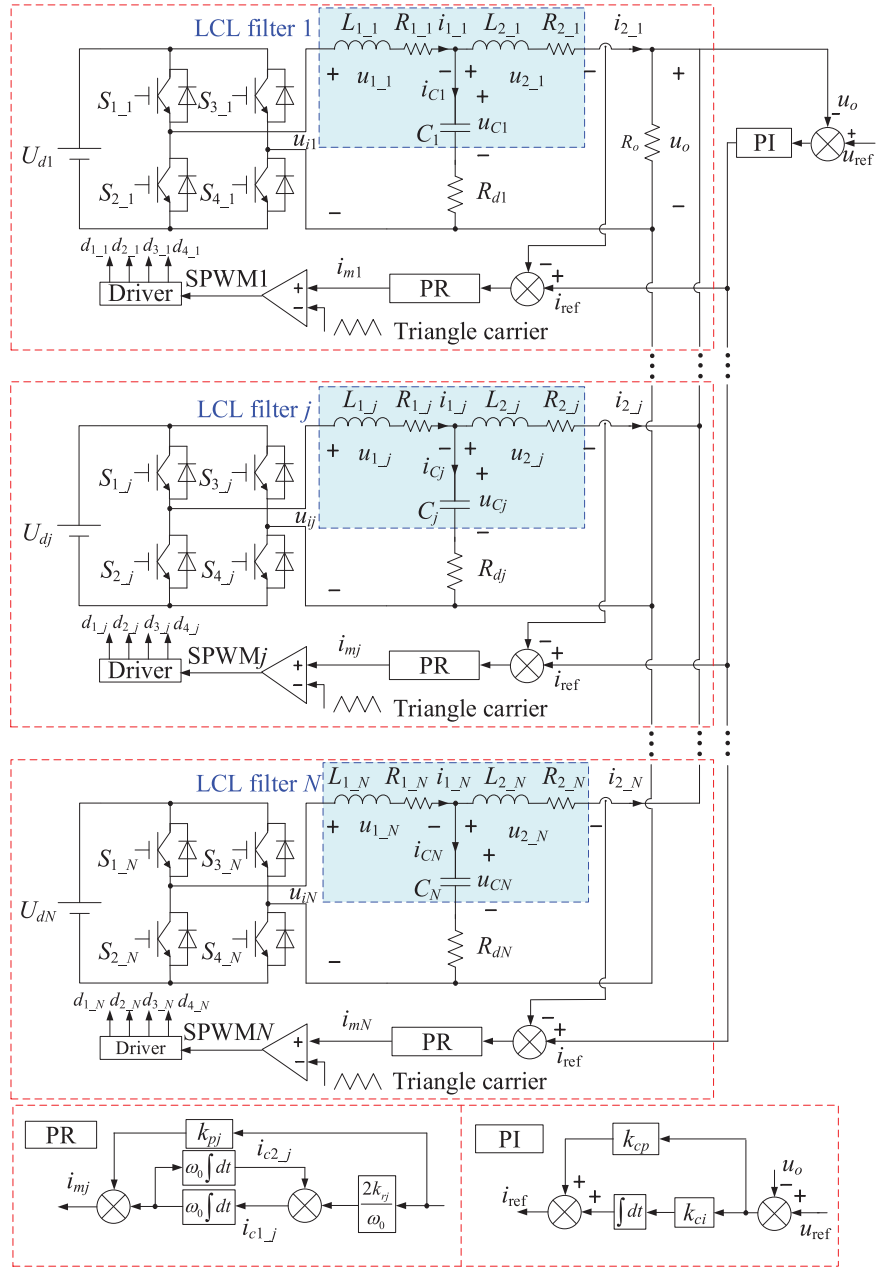


**FIGURE 7** Eigenvalues trend of  $C_2$  when increasing  $k_{cp}$  and fixed  $k_{ci} = 10$

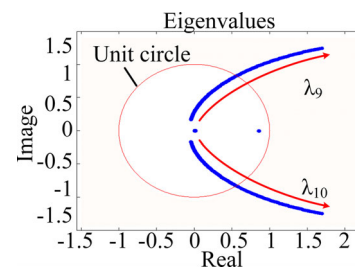


**FIGURE 8** Eigenvalues trend of  $C_2$  when increasing  $k_{ci}$  and fixed  $k_{cp} = 0.01$

stable after 0.03s, the amplitude of current can track the reference value without difference. System is stable. When  $k_{pj}(j = 1,$

$2) = 0.10$ , as shown in Figure 12, the grid-connected currents of the two inverters are resonant, the resonance peak value is



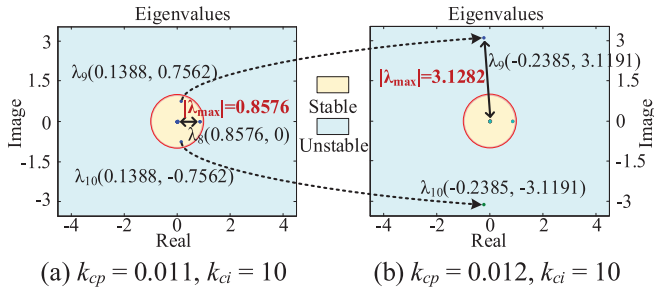


**FIGURE 9** Case I: Eigenvalue distribution of  $C_2$  when  $k_{cp}$  changing. (a)  $k_{cp} = 0.011$ ,  $k_{ci} = 10$ . (b)  $k_{cp} = 0.012$ ,  $k_{ci} = 10$

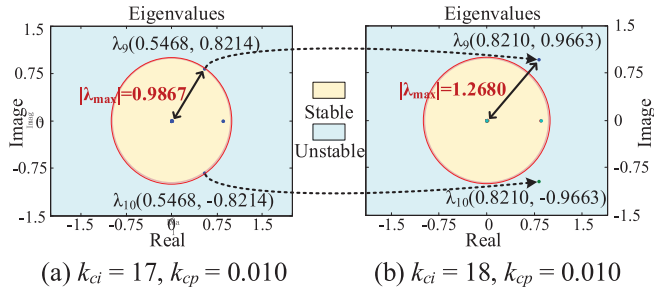


**FIGURE 10** Case II: Eigenvalue distribution of  $C_2$  when  $k_{ci}$  changing. (a)  $k_{ci} = 17$ ,  $k_{cp} = 0.010$ . (b)  $k_{ci} = 18$ ,  $k_{cp} = 0.010$

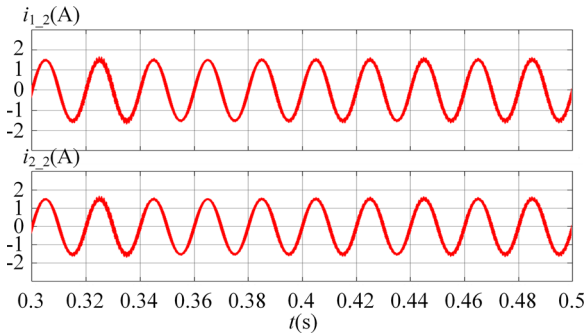


**FIGURE 11** Output current waveform of two inverters in grid-connected mode when  $k_{pj} = 0.09$ ,  $k_{rj} = 500$

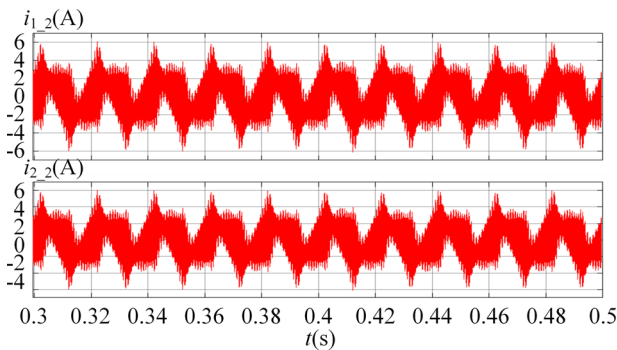


**FIGURE 12** Output current waveform of two inverters in grid-connected mode when  $k_{pj} = 0.10$ ,  $k_{rj} = 500$

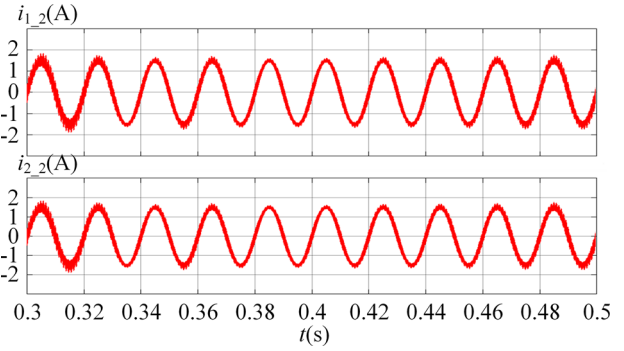


**FIGURE 13** Output current waveform of two inverters in grid-connected mode when  $k_{rj} = 530$ ,  $k_{pj} = 0.09$

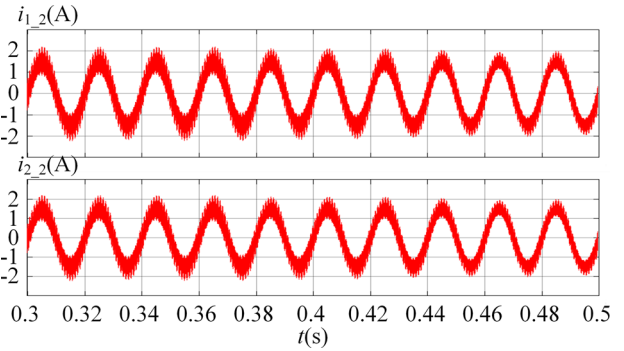


**FIGURE 14** Output current waveform of two inverters in grid-connected mode when  $k_{rj} = 540$ ,  $k_{pj} = 0.09$

greater than the reference value, the output currents of the two inverters are greatly distorted, and system is unstable.

**Case II:** It can be seen from Figure 13 that the grid-connected current of the system is stable when  $k_{rj}(j = 1, 2) = 530$ . Figure 14 depicts that the system is unstable when  $k_{rj}(j = 1, 2) = 540$ . The simulation results are almost the same with the theoretical analysis results.

#### 4.1.2 | A two-par allel inverters system in island mode

**Case I:** It can be seen from Figure 15 that the output current of the system is stable when  $k_{cp} = 0.011$ . Figure 16 depicts that the system is unstable when  $k_{cp} = 0.012$ . The simulation results are the same with the theoretical analysis results.

**Case II:** As can be obtained from Figure 17, when  $k_{ci} = 17$ , the two inverters output sinusoidal currents without oscillation, and the system is in a stable state. However, when  $k_{ci}$  increases to 18, the system has a current resonance begin from 0.08 s, as is shown in Figure 18, and according to the waveform, the system is already in an unstable state.

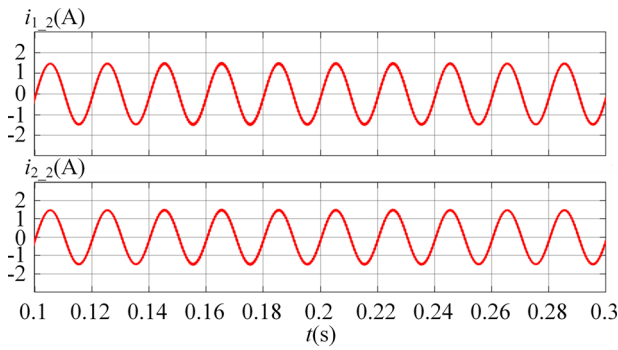


**FIGURE 15** Output current waveform of two inverters in island mode when  $k_{cp} = 0.011$ ,  $k_{ci} = 10$

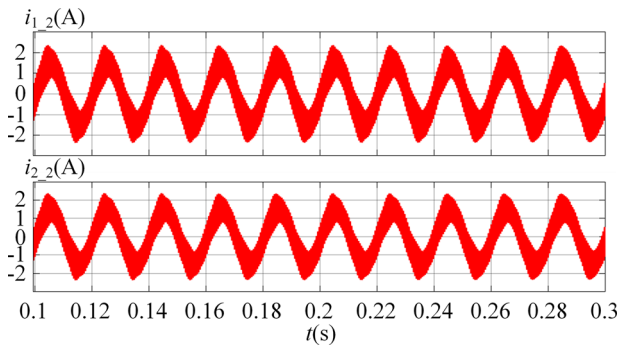


**FIGURE 16** Output current waveform of two inverters in island mode when  $k_{cp} = 0.012$ ,  $k_{ci} = 10$

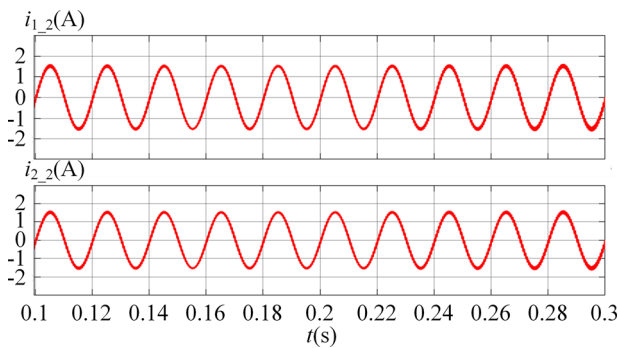


**FIGURE 17** Output current waveform of two inverters in island mode when  $k_{ci} = 17$ ,  $k_{cp} = 0.010$

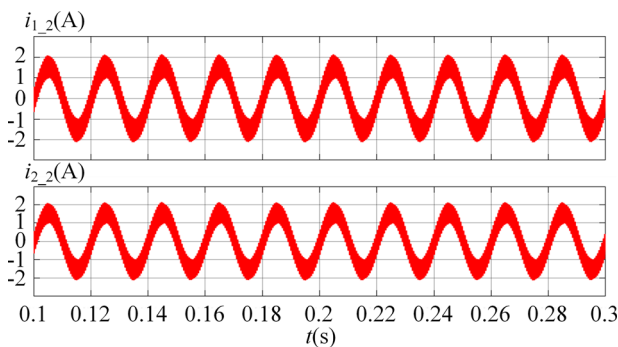


**FIGURE 18** Output current waveform of two inverters in island mode when  $k_{ci} = 18$ ,  $k_{cp} = 0.010$

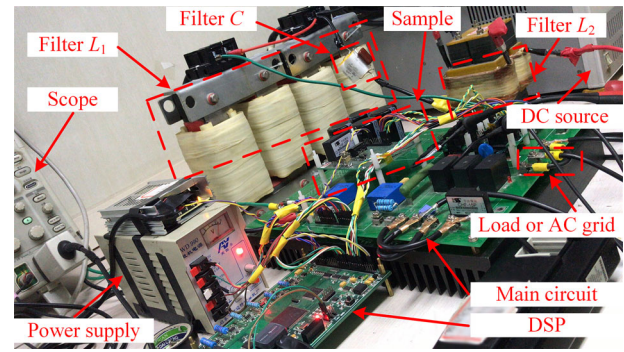


**FIGURE 19** Single-phase inverter experimental platform

**TABLE 4** The experimental specifications of single-phase inverter experimental platform

Devices	TYPE
Scope	Tektronix MSO 4054
Current probe I	Tektronix TCP 0030A
Current probe II	Tektronix TCP 0150
AC grid	Chroma 61705
DC source	Chroma 62150H-600
Load	Chroma 63204
Power supply	WD-990

## 4.2 | The experimental results

The experimental platform of the two-parallel inverters system is established, as shown in Figure 19, and the experimental specifications of the experimental platform is shown in Table 4. It should be noticed that due to the difference of probes, there is a slight difference between the blue waveform and the green waveform at the peak or trough of wave in the same image.

## 4.3 | The two-parallel inverters system in grid-connected mode

**Case I:** Increase  $k_{pj}$  gradually, as can be obtained from Figure 20, when  $k_{pj} = 0.10$ , the amplitude of the output sinusoidal current of the two inverters can track the reference value without difference, and achieve a good average current. System is stable. However, as shown in Figure 21, when the  $k_{pj}$  increases to 0.11, the output current of the two inverters resonate, the resonance peak value is greater than the reference value. System is unstable.

**Case II:** Increase  $k_{rj}$  gradually, as can be obtained from Figure 22, when  $k_{rj} = 580$ , there is no oscillation in the sinusoidal current output, and the system is in a stable state. However, when  $k_{rj}$  increases to 590, as shown in Figure 23, the system has a current resonance phenomenon, and the system is now in an unstable state.

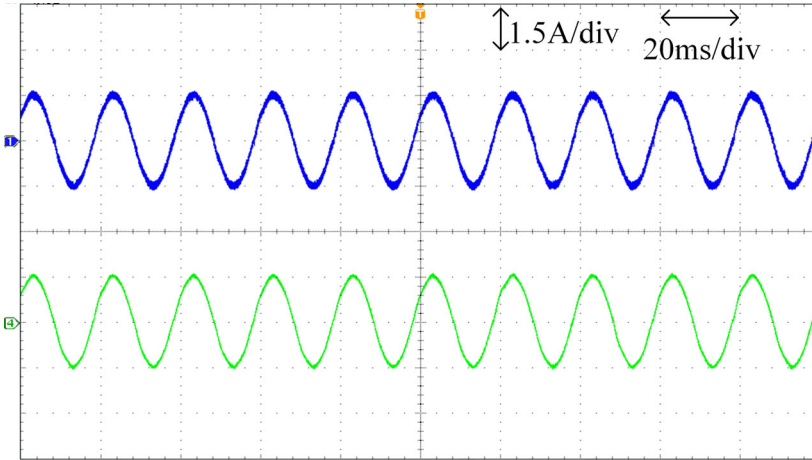


**FIGURE 20** Output current experiment waveform of two inverters in grid-connected mode when  $k_{pj} = 0.10$ ,  $k_{rj} = 500$

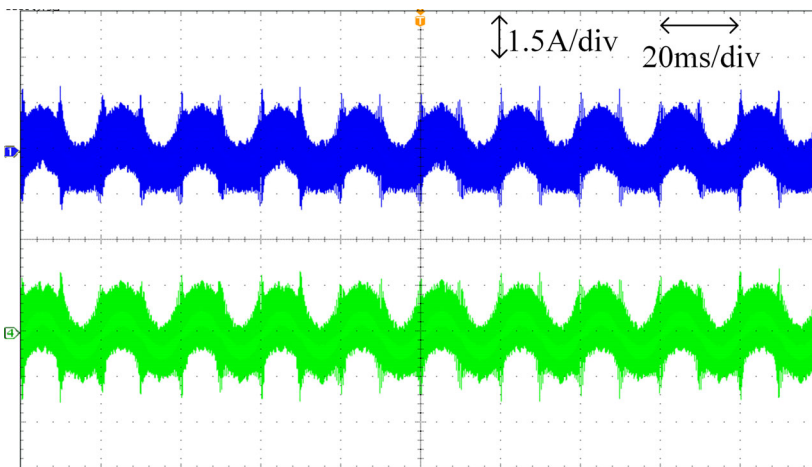


**FIGURE 21** Output current experiment waveform of two inverters in grid-connected mode when  $k_{pj} = 0.11$ ,  $k_{rj} = 500$

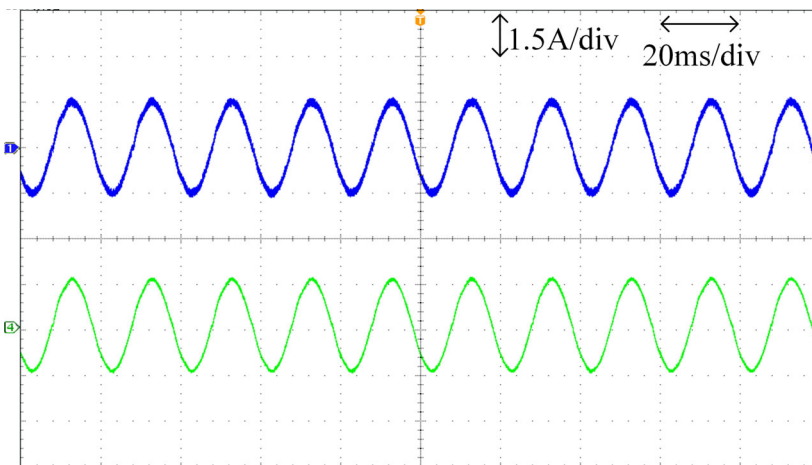


**FIGURE 22** Output current experiment waveform of two inverters in grid-connected mode when  $k_{rj} = 580$ ,  $k_{pj} = 0.09$

#### 4.4 | A two-parallel inverters system in island mode

**Case I:** Increase  $k_{\phi p}$  gradually, as can be obtained from Figure 24, when  $k_{\phi p} = 0.013$ , the amplitude of the output sinusoidal

current of the two inverters can track the reference value without difference, and achieve a good average current. System is stable. However, as shown in Figure 25, when the  $k_{\phi p}$  increases to 0.014, the output current of the two inverters resonates, the resonance peak value is greater than the reference value. System is unstable.

**FIGURE 23** Output current experiment waveform of two inverters in grid-connected mode when  $k_{rj} = 590$ ,  $k_{bj} = 0.09$

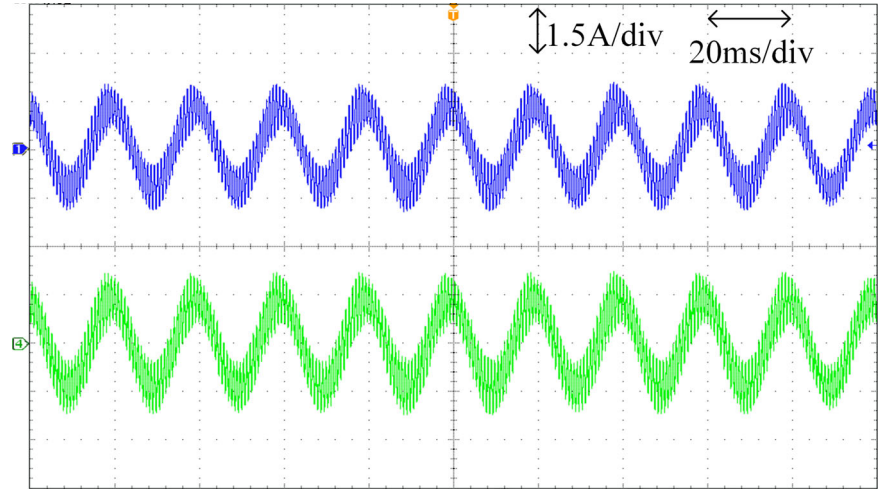


**FIGURE 24** Output current experiment waveform of two inverters in island mode when  $k_{rp} = 0.013$ ,  $k_{ip} = 10$

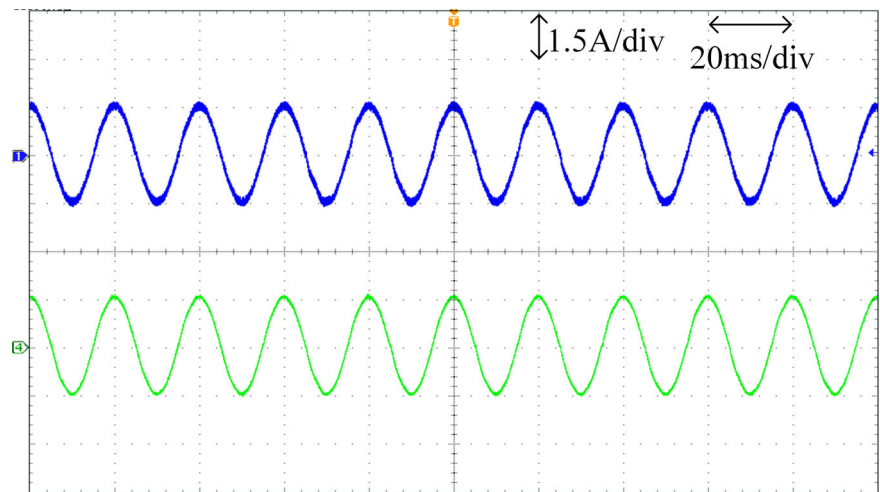
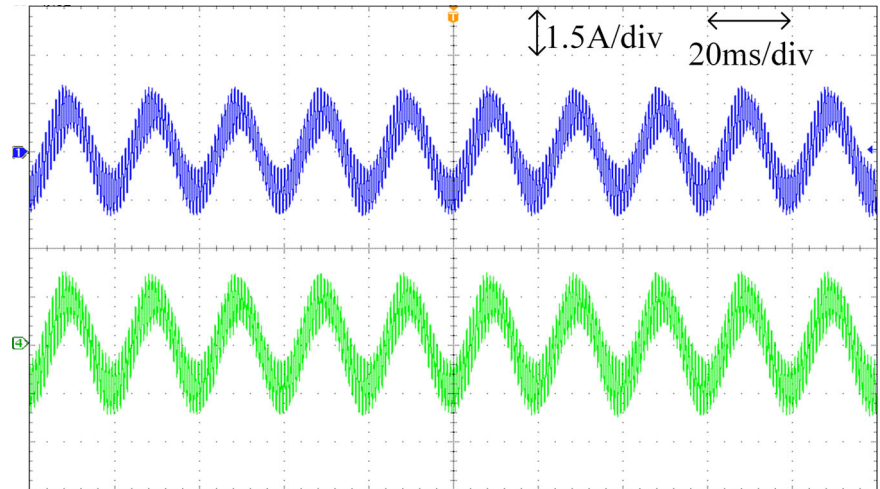


**FIGURE 25** Output current experiment waveform of two inverters in island mode when  $k_{rp} = 0.014$ ,  $k_{ip} = 10$



**Case II:** Increase  $k_{ci}$  gradually, as can be obtained from Figure 26, when  $k_{ci} = 20$ , there is no oscillation in the sinusoidal current output by the two inverters, and the system is in a stable state. However, when  $k_{ci}$  increases to 21, as shown in Figure 27, the system has a current resonance phenomenon, and the system is now in an unstable state.

In summary, although there is a slight difference caused by model simplifications, such as ignoring the stray parameters of print circuit boards and the influence of phase-locked loop, the theoretical stability analysis results, simulation and experimental results maintain good consistency, which verify the correctness of theoretical analysis.

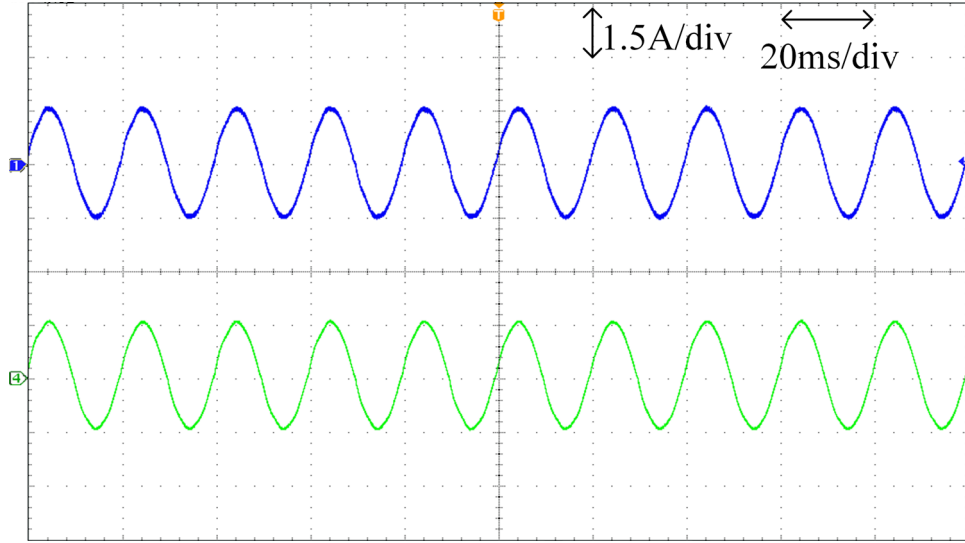


FIGURE 26 Output current experiment waveform of two inverters in island mode when  $k_{ai} = 20$ ,  $k_{cp} = 0.010$

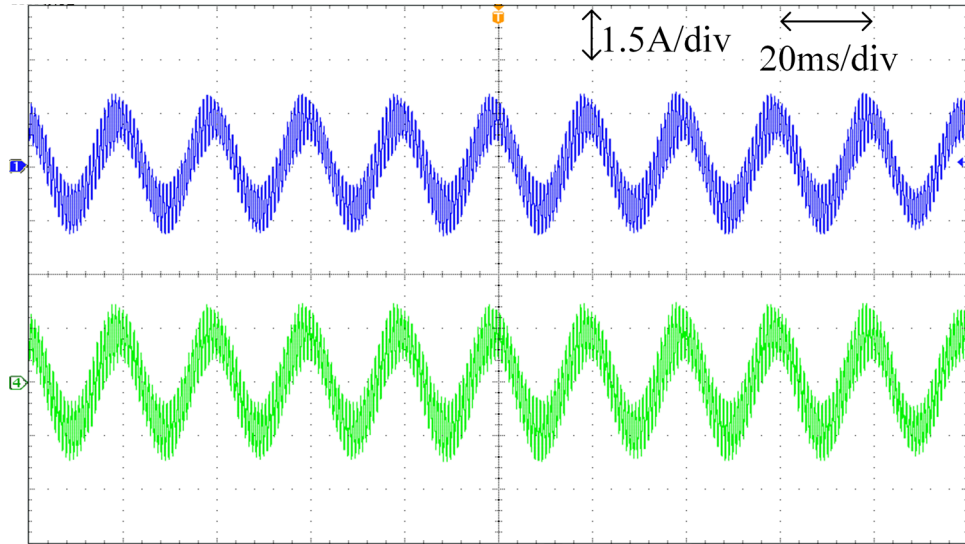


FIGURE 27 Output current experiment waveform of two inverters in island mode when  $k_{ai} = 21$ ,  $k_{cp} = 0.010$

## 5 | THE COMPLEXITY COMPARISONS

In order to prove the advantages of the proposed method over the tedious manual derivation, in this section, the complexity of  $N$ -parallel inverters stability analysis based on the Floquet criterion and the Routh criterion is compared. The manual derivation based on frequency-domain modelling is firstly conducted, then the complexity brought by the traditional frequency-domain stability analysis method and the proposed method in this paper is compared.

The  $N$ -parallel inverters system with PR control in grid-connected mode is taken as an example, as show in Figure 1. According to KCL and KVL, the power-stage transfer functions

of  $N$ -parallel inverters system can be obtained:

$$\begin{cases} u_{ij}(s) = i_{1-j}(s) \cdot (L_{1-j}s + R_{1-j}) + u_{Cj}(s) \\ i_{Cj}(s) = i_{1-j}(s) - \frac{u_{2-j}(s)}{L_{2-j}s + R_{2-j}} \\ u_{2-j}(s) = i_{Cj}(s) \cdot \left( \frac{1}{C_j s} + R_{dj} \right) - u_s(s) \\ i_s(s) = \sum_{j=1}^N [i_{2-j}(s)] \end{cases}, \quad (17)$$

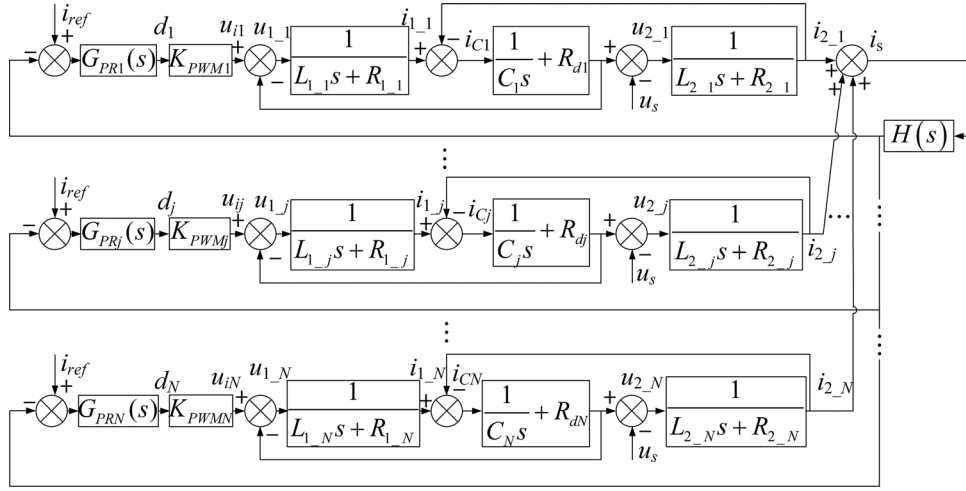


FIGURE 28 Equivalent linear transfer function block diagram of  $N$ -parallel inverters system in grid-connected mode

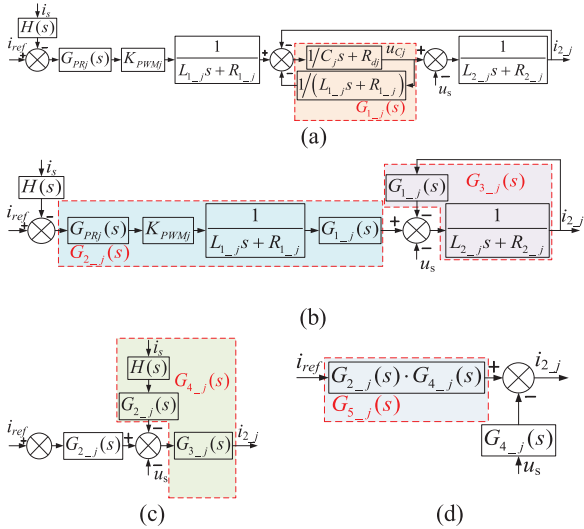


FIGURE 29 Simplify process of the transfer function block diagram. (a) Step 1. (b) Step 2. (c) Step 3. (d) Step 4

here  $j = 1, 2, \dots, N$ , and control-stage transfer functions can be obtained as also:

$$H(s) = 1/N, \quad (18)$$

$$G_{PRj}(s) = k_{pj} + \frac{2k_{rj}s}{s^2 + \omega_0^2}. \quad (19)$$

According to (17) and (19), the transfer function block diagram can be derived as shown in Figure 28. Subsequently, the transfer function block diagram can be simplified, as show in Figure 29. Finally, the expression of the system output current can be obtained as (20).

$$i_s = [G_{5-1}(s) + \dots + G_{5-j}(s) + \dots + G_{5-N}(s)] \cdot i_{ref} - [G_{4-1}(s) + \dots + G_{4-j}(s) + \dots + G_{4-N}(s)] \cdot u_s, \quad (20)$$

where  $j = 1, 2, \dots, N$  and  $k \neq j$ ,

$$G_{1-j}(s)$$

$$= \frac{L_{1-j}s + R_{1-j} + L_{1-j}R_{dj}C_j s^2 + R_{1-j}R_{dj}C_j s}{1 + R_{dj}C_j s + L_{1-j}C_j s^2 + R_{1-j}C_j s},$$

$$G_{2-j}(s)$$

$$= \frac{G_{PRj}(s) \cdot K_{PWMj} \cdot (L_{1-j}/C_j + L_{1-j}R_{dj}s + R_{1-j}/C_j s + R_{1-j}R_{dj})}{(L_{1-j}s + R_{1-j}) \cdot (L_{1-j}s + R_{1-j} + 1/C_j s + R_{dj})},$$

$$G_{3-j}(s) = \frac{1 + R_{dj}C_j s + L_{1-j}C_j s^2 + R_{1-j}C_j s}{(L_{2-j}s + R_{2-j}) \cdot (1 + R_{dj}C_j s + L_{1-j}C_j s^2 + R_{1-j}C_j s)}$$

$$+ L_{1-j}s + R_{1-j} + L_{1-j}R_{dj}C_j s^2 + R_{1-j}R_{dj}C_j s$$

$$G_{2,3-j}(s) = G_{2-j}(s) \cdot G_{3-j}(s)$$

$$= \frac{G_{PRj}(s) \cdot K_{PWMj} \cdot (1 + R_{dj}C_j s)}{(L_{2-j}s + R_{2-j}) \cdot (1 + R_{dj}C_j s + L_{1-j}C_j s^2 + R_{1-j}C_j s) + (L_{1-j}s + R_{1-j}) \cdot (1 + R_{dj}C_j s)}$$

$$G_{4-j}(s)$$

$$= \frac{G_{3-j}(s)}{H(s) \cdot [G_{2,3-1}(s) + \dots + G_{2,3-j}(s) + \dots + G_{2,3-N}(s)] + 1},$$

$$G_{5-j}(s) = G_{2-j}(s) \cdot G_{4-j}(s)$$

$$= \frac{1}{H(s) \cdot \left[ \frac{G_{2,3-1}(s)}{G_{2,3-j}(s)} + \dots + 1 + \dots + \frac{G_{2,3-N}(s)}{G_{2,3-j}(s)} \right] + \frac{1}{G_{2,3-j}(s)}}$$

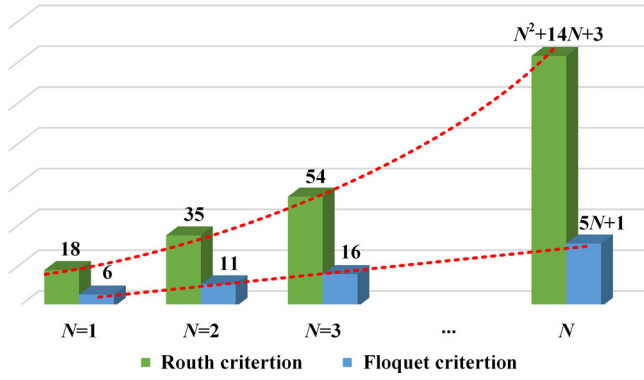


FIGURE 30 The number of formulas of  $N$ -parallel inverters stability analysis based on Floquet criterion and Routh criterion

$$G_{5\_k|j}(s) = \frac{G_{2\_3\_k}(s)}{G_{2\_3\_j}(s)}$$

$$G_{PRk}(s) \cdot K_{PWMk} \cdot (1 + R_{dk}C_k s) \cdot [(L_{1\_j}s + R_{1\_j}) \cdot (1 + R_{dj}C_j s) + (L_{2\_j}s + R_{2\_j}) \cdot (1 + R_{dj}C_j s + L_{1\_j}C_j s^2 + R_{1\_j}C_j s)]$$

$$= \frac{+ (L_{2\_j}s + R_{2\_j}) \cdot (1 + R_{dj}C_j s + L_{1\_j}C_j s^2 + R_{1\_j}C_j s)]}{G_{PRj}(s) \cdot K_{PWMj} \cdot (1 + R_{dj}C_j s) \cdot [(L_{1\_k}s + R_{1\_k}) \cdot (1 + R_{dk}C_k s) + (L_{2\_k}s + R_{2\_k}) \cdot (1 + R_{dk}C_k s + L_{1\_k}C_k s^2 + R_{1\_k}C_k s)]}$$

Since the impedance criterion only provides the sufficient condition, the stability criterion is quite conservative. Further, in practical applications, there is no clear theoretical basis for simplification but only experience. In contrast, although the closed-loop transfer function of Routh criterion is a complex high-order polynomial, it is a sufficient and necessary condition as same as Floquet theory. Therefore, the Routh criterion is instanced to compare with the proposed method in this paper.

Flowchart of  $N$ -parallel inverters stability analysis based on Floquet criterion and Routh criterion is given in Figure 30. For the stability analysis of  $N$ -parallel system based on Routh criterion, there are six steps and  $N^2 + 14N + 3$  formulas, including  $3N + 1$  power-stage frequency-domain equations,  $N + 1$  control-stage frequency-domain equations,  $6N + N(N - 1)$  simplified frequency-domain transfer function which are caused by the interaction among inverter modules, and  $5N + 1$  coefficients of Routh Table. In contrast, for the stability analysis based on Floquet criterion, there are only four steps and  $5N + 1$  formulas, including  $3N + 1$  power-stage time-domain differential equations and  $2N$  control-stage time-domain differential equations.

On the other hand, different from Floquet criterion, to determine the stability of the system based on the traditional Routh criterion, the characteristic equation of the closed-loop

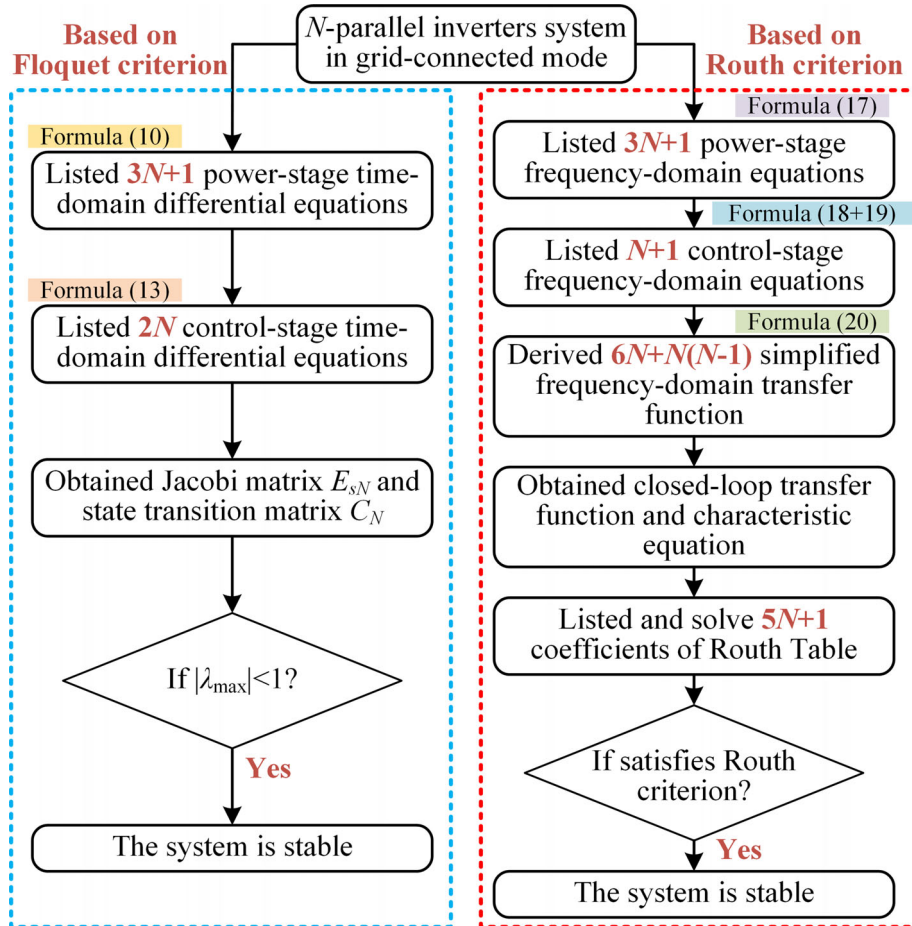


FIGURE 31 Flowchart of  $N$ -parallel inverters stability analysis based on Floquet criterion and Routh criterion

**TABLE 5** Complexity comparisons of  $N$ -parallel inverters stability analysis based on Floquet criterion and Routh criterion

Criterion name	Number of steps	Number of formulas	When $N \geq 3$
Floquet	4	$5N+1$	Feasible
Routh	6	$N^2+14N+3$	Infeasible

transfer function of the system needs to be obtained, namely, it is necessary to standardise closed-loop transfer function. However, since the simplification of the frequency-domain transfer function has no rules to follow, the standardisation process is extremely complicated. Hence, for the parallel system with  $N \geq 3$ , the stability analysis based on the Routh criterion is completely infeasible.

Based on the Flowchart in Figure 30, complexity comparisons of  $N$ -parallel inverters stability analysis based on Floquet criterion and Routh criterion can be summarised, as show in Table 5 and Figure 31. It is clear that Routh criterion requires more steps and formulas, and as the number  $N$  of parallel inverters in the system increasing, the number of formulas increases at quadratic growth coefficients. Therefore, Floquet criterion is more suitable for analysing the stability of complex systems than Routh criterion.

## 6 | CONCLUSIONS

This paper provides a simple and fast stability analysis method for  $N$ -parallel inverters systems. Aiming at  $N$ -parallel inverters system with the PR control and the average current control, a general time-domain model is established. Taking a 2-parallel inverters system as an example, the correctness of the proposed method is verified based on simulations and experiments, both for grid-connected mode and for island mode; further, the result of complexity comparisons show that the proposed time-domain method has advantages over traditional frequency-domain method in terms of time consumption, both in number of steps and number of formulas. These mean that the derived general time-domain model with the corresponding stability criterion based on the Floquet theory is effective and is more suitable for a complex  $N$ -parallel inverters system. Hence, this paper provides a new fast stability analysis method for  $N$ -parallel inverters system.

## ACKNOWLEDGEMENTS

This work was supported in part by the Excellent Youth Scholars of National Natural Science Foundation of China under Grant 51822701, in part by the key project of National Natural Science Foundation of China under Grant U1866211, in part by the General Programs of the National Natural Science Foundation of China under Grants 51577010, 51777012 and in part by the Fujian Provincial Natural Science Foundation under the grant Nr. 2020J01800.

## CONFLICT OF INTEREST

The authors declare no conflict of interest.

## ORCID

Hong Li  <https://orcid.org/0000-0002-8117-8980>

## REFERENCES

- Komurcugil, H., Bayhan, S., Abu-Rub, H.: Lyapunov-function based control approach with cascaded PR controllers for single-phase grid-tied LCL-filtered quasi-Z-source inverters. 2017 11th IEEE International Conference on Compatibility, Power Electronics and Power Engineering (CPE-POWERENG), Cadiz, pp. 510–515 (2017)
- Shen, G., Zhu, X., Zhang, J., Xu, D.: A new feedback method for PR current control of LCL-filter-based grid-connected inverter. IEEE Trans. Ind. Electron. 57(6), 2033–2041 (2010)
- Alemi, P., Bae, C., Lee, D.: Resonance suppression based on PR control for single-phase grid-connected inverters with LCL filters. IEEE J. Emerg. Sel. Topics Power Electron. 4(2), 459–467 (2016)
- He, J., Li, Y.W., Bosnjak, D., Harris, B.: Investigation and active damping of multiple resonances in a parallel-inverter-based microgrid. IEEE Trans. Power Electron. 28(1), 234–246 (2013)
- Weibin, Y., Liansong, X., Tao, Z.: Review of stability analysis methods of grid-tied inverter power generation systems. Southern Power Syst. Technol. 13(01), 14–26 (2019)
- Monopoli, V.G., et al.: Applications and modulation methods for modular converters enabling unequal cell power sharing: carrier variable-angle phase-displacement modulation methods. IEEE Industrial Electronics Magazine, pp. 2–13 (2021)
- Rivera, S., Kouro, S., Vazquez, S., Goetz, S.M., Lizana, R., Romero-Cadaval, E.: Electric vehicle charging infrastructure: from grid to battery. IEEE Ind. Electron. Mag. 15(2), 37–51 (2021)
- Wang, S., Liu, Z., Liu, J., Boroyevich, D., Burgos, R.: Small-signal modeling and stability prediction of parallel droop-controlled inverters based on terminal characteristics of individual inverters. IEEE Trans. Power Electron. 35(1), 1045–1063 (2020)
- Wang, Y., Han, X., Zhang, B., Kong, J., Li, C., Ren, C.: Analysis of interaction among multiple parallel three-phase grid-connected inverters based on RGA. 2020 IEEE 9th International Power Electronics and Motion Control Conference (IPEMC2020-ECCE Asia), Nanjing, China, pp. 2472–2479 (2020)
- Enslin, J.H.R., Heskes, P.J.M.: Heskes: harmonic interaction between a large number of distributed power inverters and the distribution network. IEEE Trans. Power Electron. 19(6), 1586–1593 (2004)
- Wang, X., Blaabjerg, F., Wu, W.: Modeling and analysis of harmonic stability in an AC power-electronics-based power system. IEEE Trans. Power Electron. 29(12), 6421–6432 (2014)
- Wang, F., Duarte, J.L., Hendrix, M.A.M., Ribeiro, P.F.: Modeling and analysis of grid harmonic distortion impact of aggregated DG inverters. IEEE Trans. Power Electron. 26(3), 786–797 (2011)
- Wang, X., Blaabjerg, F., Liserre, M., Chen, Z., He, J., Li, Y.: An active damper for stabilizing power-electronics-based AC systems. IEEE Trans. Power Electron. 29(7), 3318–3329 (2014)
- Middlebrook, R.D.: Input filter considerations in design and application of switching regulators. IEEE Industrial Application Social Annual Meeting, pp. 336–382 (1976)
- Wildrick, C.M., Lee, F.C., Cho, B.H., Choi, B.: A method of defining the load impedance specification for a stable distributed power system. IEEE Trans. Power Electron. 10(3), 280–285 (1995)
- Feng, X., Liu, J., Lee, F.C.: Impedance specifications for stable DC distributed power systems. IEEE Trans. Power Electron. 17(2), 157–162 (2002)
- Li, H., et al.: An extended stability analysis method for paralleled DC-DC converters system with considering the periodic disturbance based on Floquet theory. IEEE Access 8, 9023–9036 (2020)
- Liu, Z., Liu, J., Hou, X., Dou, Q., Xue, D., Liu, T.: Output impedance modeling and stability prediction of three-phase paralleled inverters with master-slave sharing scheme based on terminal characteristics of individual inverters. IEEE Trans. Power Electron. 31(7), 5306–5320 (2016)
- He, J., Li, Y.W.: Analysis, design, and implementation of virtual impedance for power electronics interfaced distributed generation. IEEE Trans. Ind. Appl. 47(6), 2525–2538 (2011)



20. Sun, J.: Small-signal methods for AC distributed power systems—a review. *IEEE Trans. Power Electron.* 24(11), 2545–2554 (2009)
21. Ogata, K.: *Modern Control Engineering*. Publishing House of Electronics Industry, Beijing (2011)
22. Bian, J., Li, H., Zheng, T.Q.: Stability analysis of grid-connected inverters with LCL-filter based on harmonic balance and Floquet theory. 2014 International Power Electronics Conference (IPEC-Hiroshima 2014 - ECCE ASIA), Hiroshima, pp. 3314–3319 (2014)
23. Wang, Y., Wang, X., Chen, Z., Blaabjerg, F.: State-space-based harmonic stability analysis for paralleled grid-connected inverters. *IECON 2016 - 42nd Annual Conference of the IEEE Industrial Electronics Society*, Florence, Italy, pp. 7040–7045 (2016)
24. Pogaku, N., Prodanovic, M., Green, T.C.: Green: modeling, analysis and testing of autonomous operation of an inverter-based microgrid. *IEEE Trans. Power Electron.* 22(2), 613–625 (2007)
25. Bottrell, N., Prodanovic, M., Green, T.C.: Dynamic stability of a microgrid with an active load. *IEEE Trans. Power Electron.* 28(11), 5107–5119 (2013)
26. Han, Y., et al.: Floquet-theory-based small-signal stability analysis of single-phase asymmetric multilevel inverters with SRF voltage control. *IEEE Trans. Power Electron.* 35(3), 3221–3241 (2020)
27. Burton, T.A., Muldowney, J.S.: A generalized floquet theory. *Archiv Der Mathematik.* 19(2), 188–194 (1968)
28. Wang, F., Zhang, H., Ma, X.: Analysis of slow-scale instability in boost PFC converter using the method of harmonic balance and Floquet theory. *IEEE Trans. Circuits Syst. I Regul. Pap.* 57(2), 405–414 (2010)
29. Li, H., Guo, Z., Ren, F., Zhang, X., Zhang, B.: A stability analysis method based on Floquet theory for multi-stage DC-DC converters system. 2017 IEEE Energy Conversion Congress and Exposition (ECCE), Cincinnati, OH, pp. 3025–3029 (2017)
30. Li, H., Liu, C., Jiang, X., Zeng, Y., Guo, Z., Zheng, T.Q.: A time-domain stability analysis method for grid-connected inverter with PR control based on Floquet theory. *IEEE Trans. Ind. Electron.* 68, 11125–11134 (2021)
31. Cheng, P., Ding, G., Song, C., Chai, H., Xu, G.: Stability analysis of identical paralleled DC-DC converters with average current sharing. 2019 IEEE Asia Power and Energy Engineering Conference (APEEC), Chengdu, China, pp. 60–64 (2019)
32. Chandorkar, M.C., Divan, D.M., Adapa, R.: Control of parallel connected inverters in standalone AC supply systems. *IEEE Trans. Ind. Appl.* 29(1), 136–143 (1993)
33. Guerrero, J.M., de Vicuna, L.G., Matas, J., Castilla, M., Miret, J.: A wireless controller to enhance dynamic performance of parallel inverters in distributed generation systems. *IEEE Trans. Power Electron.* 19(5), 1205–1213 (2004)
34. Dragicevic, T., Vazquez, S., Wheeler, P.: Advanced control methods for power converters in DG systems and microgrids. *IEEE Trans. Ind. Electron.* 68, 5847–5862 (2019)
35. Generators connected to the LV distribution network—technical requirements for the connection to and parallel operation with low-voltage distribution networks. VDE-AR-N 4105, Verband der Elektrotechnik (2011)
36. Yang, Y., et al.: Reactive power injection strategies for single-phase photovoltaic systems considering grid requirements. *IEEE Trans. Ind. Appl.* 50, 4065–4076 (2014)
37. Freddy, T.K.S., et al.: Modulation technique for single-phase transformerless photovoltaic inverters with reactive power capability. *IEEE Trans. Ind. Electron.* 64, 6989–6999 (2017)

**How to cite this article:** Li, H., Jiang, X., Liu, C., Li, Z., Franquelo, L.G., Vazquez, S.: A Floquet theory-based fast time-domain stability analysis for  $N$ -parallel inverters system. *IET Power Electron.* 15, 186–202 (2022). <https://doi.org/10.1049/pel2.12225>